On the Influence of Site Pairing in Hydrophobic Silica-Supported Sulfonic Acid Bifunctional Catalysts

Journal:	*Langmuir*
Manuscript ID	la-2020-00312t
Manuscript Type:	Article
Date Submitted by the Author:	03-Feb-2020
Complete List of Authors:	Kasinathan, Palraj; Université catholique de Louvain Lang, Charlotte; Université catholique de Louvain Gaigneaux, Eric; Universite catholique de Louvain, Institute of Condensed Matter and Nanosciences Jonas, Alain; Universite catholique de Louvain, IMCN/BSMA Fernandes, Antony; Université catholique de Louvain,

On the Influence of Site Pairing in Hydrophobic Silica-Supported Sulfonic Acid Bifunctional Catalysts

Palraj Kasinathan,[a] Charlotte Lang,[a] Eric M. Gaigneaux,[a] Alain M. Jonas,[a] and Antony E. Fernandes*[a],[b]

[a] Institute of Condensed Matter and Nanosciences, Bio- and Soft Matter, Université catholique de Louvain, 1348 Louvain-la-Neuve, Belgium

[b] Certech, Rue Jules Bordet 7180 Seneffe, Belgium

ABSTRACT: Imparting hydrophobicity to solid acid catalysts is critical to regulate their performances by allowing the creation of less polar environment and improved partitioning of the reactants. Here we present different approaches for the preparation of silica-based catalysts comprising sulfonic acid (-SO_3H) sites and hydrophobic decyl (-C_{10}) chains either by simultaneous or sequential post-functionalization of an azide-functionalized mesoporous silica platform. This set of hybrid bifunctional catalysts are compared in the model esterification of octanol with acetic acid, and the influence of the preparation methods together with the resulting site spatial distribution are discussed. In parallel, we show that pairing the two functional groups affords a maximum synergistic effect compared to more traditional mixed-catalysts with random distributions of acid and hydrophobic functions.

INTRODUCTION

Porous solid acid catalysts are crucial for the valorization of renewable biomass. Yet, typical heterogeneous acid catalysts, which are by essence highly hydrophilic by virtue of their surface active sites and from their support framework, are not well suited for the conversion of bio-based feedstock that often includes fatty or high-water content reactants. Additionally, an important part of the transformations involved in the conversion of biomass, such as dehydrations or esterifications, induces the formation of water as a by-product that also contributes to the deactivation of the active sites. There

is therefore an urgent need to find methods to adjust the surface hydrophobicity of solid acid catalysts to enhance the partitioning of the reactants and to displace water from the active sites.[1-2]

In this direction, mesoporous silica-supported sulfonic acid catalysts are particularly interesting owing to the possibility to access a wide range of materials with tunable porosity and co-functionality to improve mass transport and surface properties. Especially, numerous efforts have been developed to impart hydrophobicity to conventional propylsulfonic acid silicas (Si-PrSO_3H) either by modification on the surface or in the walls of the silica matrix. Typically, simple capping of the residual silanols with trimethylsilyl groups can already provide enhanced activity.[3-5] Another possibility for the preparation of hydrophobic sulfonic acid silicas is by the co-condensation of the mercapto-terminated alkoxysilane, precursor of the sulfonic acid site, with an alkyl-alkoxysilane (*e.g.*, methyl, ethyl, propyl, octyl, phenyl).[6-8] This affords a rapid entryway to adjust the hydrophilic/hydrophobic balance by controlling the molar ratio of the two silanes in the co-condensation. Similarly, post-synthesis grafting can also be used to insert hydrophobic organic groups on Si-PrSO_3H or its unoxidized Si-PrSH precursor.[8-12] In another way, hydrophobicity can be introduced directly from siliceous precursors leading to periodic mesoporous organosilicas (PMOs)[13-19] incorporating hydrophobic organic bridging groups (e.g., phenyl) in their framework, that are then grafted with sulfonic acid sites.[20-26]

We recently reported a versatile post-modification method to adjust both the acid strength and surface polarity of sulfonic acid silicas (Scheme 1a).[27] In this approach, the sulfonic acid group is first grafted on azide-functionalized mesoporous silica using the copper-catalyzed azide-alkyne cycloaddition (CuAAC) chemistry, and the obtained triazole linker is further used to attach secondary functional groups by nucleophilic substitution (this can also be reversed, i.e., CuAAC-grafting of the secondary groups followed by insertion of the sulfonic acid on the formed triazole). Therefore, this method gives access to unique hybrid bifunctional catalysts with paired organic groups, in contrast with current surface modification schemes that provide mixed monolayers with random spatial distribution of the functional groups.

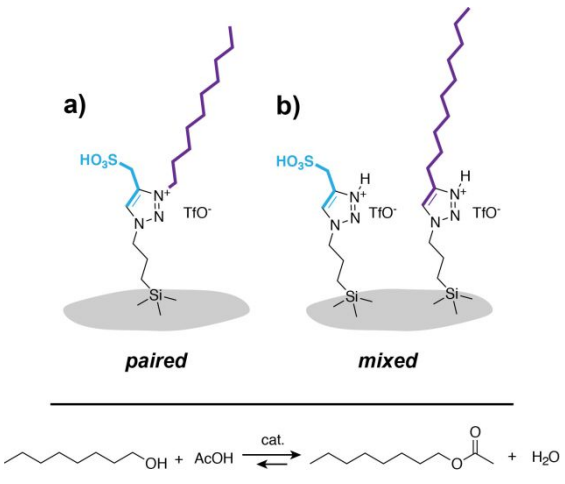

Scheme 1. (a) Paired and (b) mixed bifunctional silica-supported hydrophobic acid catalysts bearing sulfonic acid (-SO_3H) and decyl (-C_{10}) sites studied in the esterification of octanol with acetic acid.

Given the importance of spatial distribution of surface groups in multifunctional cooperative or synergistic catalysis,[28-37] we anticipated that our methodology, which affords a unique control on the relative location of hydrophobic moieties and acid sites, would be of significance in the search for more efficient silica-supported sulfonic acid catalysts.

Here, we report novel post-functionalization methods to obtain, with good accuracy, hybrid bifunctional sulfonic acid silicas comprising pre-determined SO_3H/C_{10} surface ratios based on CuAAC (Scheme 1b). We also demonstrate that the spatially-controlled coupling of the synergistic sites through the triazole link (Scheme 1a), albeit obviously limited to a 1:1 molar ratio on surface, brings a significant improvement over the series of mixed-monolayer catalysts with assumed random spatial distribution, providing insight on the impact of functional group pairing in supported synergistic catalysis.

EXPERIMENTAL SECTION

General considerations

Reagents were obtained from commercial sources and used without further purification. All reactions were carried out under argon. The azide-functionalized silica and Si-paired were prepared as described previously.[27] Spherical silica gel (40-75 μm, 100 Å) was purchased from Sorbtech Technologies. Milli-Q water (resistivity 18.2 MΩ.cm) was

obtained from a Milli-Q Reference system (Merck). FT-IR was measured on a Thermo Scientific FT-IR Nexus 870 spectrometer. TGA was measured on a Mettler Toledo TGA/SDTA 851e instrument. The weight loss was measured in the 150-900°C temperature range. Specific surface area and pore size were obtained through nitrogen adsorption-desorption experiments using a Micromeritics Tristar 3000. Before analysis, the samples were degassed overnight under vacuum at 150°C. BET and BJH approaches were applied to process the raw data. X-ray photoelectron spectroscopy (XPS) measurements were performed on a SSX 100/206 photoelectron spectrometer from Surface Science Instruments equipped with a monochromatized microfocused Al X-ray source (1486.6 eV operated at 20 mA and 10 kV). All binding energies are referenced to the C-(C, H) component of the C 1s peak fixed at 284.8 eV. The base pressure in the spectrometer was in the low 10^{-8} Torr range. Peak decomposition was achieved with Casa XPS (Casa Software Ltd., UK). Elemental analysis was performed on an EL cube apparatus. GC was performed on a Varian 3800 apparatus equipped with a CP-Sil8 CB column (30 m×0.25 mm×0.1 µm) and FID detector.

Preparation of monofunctional silica Si-1-7

Azide-functionalized silica was suspended in EtOH/water (2:1, 20 mL/g). The alkyne (1.5 to 3.0 equiv.) was added subsequently followed by sodium ascorbate (0.75 equiv.) and $CuSO_4$ (0.625 equiv.). The reaction was stirred overnight at rt/65°C (depending on the alkyne boiling point) and monitored by FT-IR and TGA. The functionalized silica was recovered by filtration and washed with DMF, water, 2 M HCl, MeOH and CH_2Cl_2 and dried in vacuum at 60°C overnight.

Simultaneous preparation of bifunctional Si-sim-x

Azide-functionalized silica was suspended in EtOH/water (2:1, 20 mL/g). Sodium propargylsulfonate **1** and 1-dodecyne **7** (in proportions shown in Table 2) were added and the reaction stirred 30 min. Sodium ascorbate (0.75 equiv.) and $CuSO_4$ (0.625 equiv.) were added and the reaction was stirred overnight at 65°C and monitored by FT-IR and TGA. The functionalized silica was recovered by filtration and washed with DMF, water, 2 M HCl, MeOH and CH_2Cl_2 and dried overnight in vacuum at 60°C.

Sequential preparation of bifunctional Si-seq-x

Azide-functionalized silica was suspended in EtOH/water (2:1, 20 mL/g). Sodium propargylsulfonate (x equiv., see Table 3) was added subsequently followed by sodium ascorbate (0.75 equiv.) and $CuSO_4$ (0.625 equiv.). The reaction was stirred overnight at 65°C and monitored by FT-IR and TGA. The functionalized silica was recovered by filtration and washed with DMF, water, 2 M HCl, MeOH and CH_2Cl_2 and dried overnight in vacuum at 60°C. The obtained silica was then suspended in degassed DMF (15 mL/g). 1-Dodecyne (1.5 equiv.) was added subsequently followed by Et_3N (5 equiv.) and CuI (0.1 equiv.). The reaction was stirred overnight at 65°C and monitored by FT-IR and TGA. The functionalized silica was recovered by filtration and washed with DMF, water, 2 M HCl, MeOH and CH_2Cl_2 and dried overnight in vacuum at 60°C.

Treatment with TfOH

The functional silica was suspended in CH_2Cl_2 (20 mL/g). TfOH (1.05 equiv.) was added and the reaction was stirred at room temperature for 4 h. The functionalized silica was recovered by filtration, washed with CH_2Cl_2 and dried overnight in vacuum at 60°C.

Ion-exchange capacity

Ion-exchange capacity (IEC) was determined by acid-base titration. Typically, the functionalized silica (ca. 100 mg) was dispersed in 2 M NaCl (10 mL) and stirred at 20°C for 1 day. After decantation, the resulting solution was titrated with 5 mM NaOH in presence of phenolphthalein as an indicator.

Potentiometric titration

Potentiometric titration was performed with Hanna HI 991002 Digital pH-mV model using a pH/ORP electrode. The dry solid catalysts (ca. 100 mg) was suspended in acetonitrile (10 mL) and agitated for 3 h. The suspension was then titrated with 5 mM *n*-butylamine.

Catalysis

The esterification reactions were carried out in a 50 mL round-bottom flask equipped with a reflux condenser. Before the reaction, the catalysts were activated at 105°C for 6 h. The conversions were determined by GC analysis using reference samples. The initial

reaction rates were determined by fitting the corresponding experimental data at low conversions with a linear function passing through the origin. In a typical run, acetic acid (5.54 g, 0.09 mol) and the catalyst (0.1 mol%) were charged into the flask and heated to the reaction temperature (83°C). On attaining the desired temperature, *n*-octanol (4 g, 0.03 mol) was introduced into the reaction mixture and this moment was considered as the zero reaction time. Samples were collected at regular intervals and analyzed by gas chromatography.

RESULTS AND DISCUSSION

Selection of the hydrophobic secondary group

A series of functional alkynes were initially screened to determine their potential to balance the hydrophilicity of silica surfaces. This comprised linear alkyl, phenyl, *tert*-butyl and fluorinated alkynes (Scheme 2).

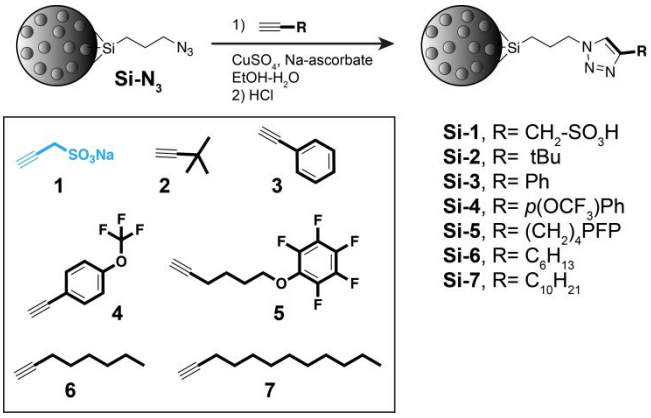

Scheme 2. CuAAC-grafting of secondary hydrophobic groups on mesoporous silica.

As we aimed at preparing mixed monolayers (Scheme 1b) using simultaneous grafting of the sulfonate and hydrophobic groups, it is important that both groups react on surface under identical CuAAC conditions previously optimized for propargylsulfonate **1**.[27] Hence, secondary alkynes **2**-**7** were individually grafted on azide-functionalized mesoporous silica **Si-N$_3$** under typical CuAAC conditions used for **1**. Thermogravimetric analysis (TGA) (Figure S1) and FT-IR (Figure S5) of silicas **Si-1-7** confirmed the efficient covalent grafting with efficiencies between 80 and 100% (Table 1). In parallel, the grafting was also performed on azide-functionalized silicon wafers to evaluate the

hydrophobic potential of the secondary groups by water contact angle (WCA) measurements (Figure S9). From this, it appeared that the decyl and trifluoro groups imparted maximum hydrophobicity (WCA *ca.* 75°) in contrast with the sulfonic acid-functionalized sample (WCA= 31°) (Table 1). Noteworthy, the pentafluorophenyl (PFP) group, although providing notable surface hydrophobicity (WCA= 66°), was obtained with moderate grafting efficiency (84%) and was not thermally stable enough as observed by TGA (Figure S1). For simplicity and commercial availability, alkyne **7** with a decyl group was selected over **4** for pursuing the study.

Table 1. Organic loading and water contact angle (WCA) for silicas **Si-1-7**.

Silica	Organic loading (mmol/g)[a]	Grafting efficiency (%)[a]	WCA (°)[b]
Si-N_3	0.31	-	64 ±1
Si-1	0.31	100	31 ±2
Si-2	0.27	87	55 ±1
Si-3	0.29	94	55 ±1
Si-4	0.29	94	78 ±1
Si-5	0.26	84	66 ±1
Si-6	0.31	100	55 ±1
Si-7	0.31	100	75 ±1

[a] Measured on modified mesoporous silica; [b] measured on modified silicon wafers

Remarkably, as both hydrophilic propargylsulfonate **1** and the more hydrophobic 1-dodecyne **7** "click" under same CuAAC conditions on azide silica, it is possible to envision their direct co-grafting. Following this approach, we previously demonstrated that it is possible to control the final surface ratio of the functional groups by tuning their molar ratio in the grafting solution, provided that no large excess of alkynes is used compared to the azide loading.[38-39] Hence, bifunctional silicas **Si-sim-x** (with x the SO_3/C_{10} solution ratio) were prepared in one step starting from different solution ratios of **1** and **7**, using a total of 1.2 equiv. of alkynes compared to the azide loading (Scheme 3, Table 2).

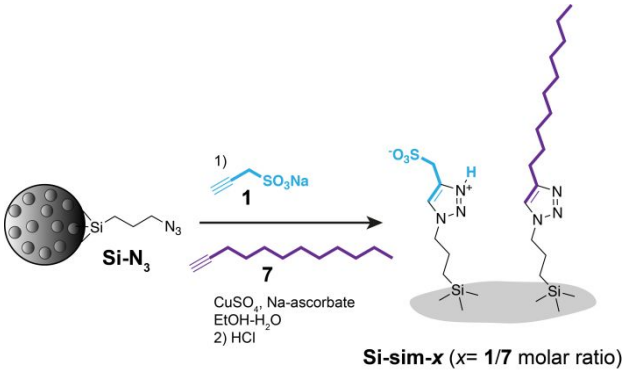

Scheme 3. Simultaneous preparation of bifunctional mixed SO_3/C_{10} silica.

The surface contents in sulfonic acid and decyl groups were determined by ion exchange capacity (IEC) measurements and TGA (Figure S2), respectively (Table 2); it appeared however difficult to obtain complete grafting under these conditions, with 10-40% of azide groups being left unreacted on surface, as confirmed by FT-IR that revealed residual azide functions at 2100 cm^{-1}.

Table 2. Determination of surface ratios for silicas **Si-sim-*x***.

Silica	**1/7** molar ratio in solution	IEC (mmol H^+/g)	Total organic loading (mmol/g)	SO_3/C_{10} surface ratio	Grafting efficiency (%)
Si-N_3	-	0.04	0.37	-	-
Si-sim-0.5	0.5	0.09	0.34	0.17	92
Si-sim-1.0	1.0	0.15	0.37	0.39	100
Si-sim-2.0	2.0	0.17	0.27	0.91	73
Si-sim-5.0	5.0	0.22	0.26	2.26	70
Si-sim-20.0	20.0	0.24	0.22	8.14	59

Remarkably, the derivative thermogravimetry (DTG) curves (Figure S2) confirmed the presence of both -SO_3H and -C_{10} sites in the mixed catalysts **Si-sim-x** wherein thermal events corresponding to both monofunctional **Si-1** (-SO_3H, 350°C) and **Si-7** (-C_{10}, 400°C) could be observed with different amplitude as a function of the ratio of alkynes **1** and **7** in the grafting solutions. DTG also evidenced incomplete grafting in some instances, with thermal event corresponding to the residual azide layer (250°C). XPS also verified the presence of a S 2s signal at 232.2 eV consistent with oxidized sulfur (Figure S12).

Kinetic study (Figure 1a) revealed that, although **1** and **7** graft under similar rates on azide silica, an excess of **1** is necessary to achieve its quantitative grafting (Figure 1b). Consequently, this results in incomplete grafting and surface ratios deviating from solution ratios in mixed catalysts **Si-sim-x** (Table 2). From these data, it is possible to predict the theoretical SO_3/C_{10} surface ratio as a function of the ratio of alkynes **1**/**7** in solution that indeed fitted well with the experimental ratios (Figure 1c).

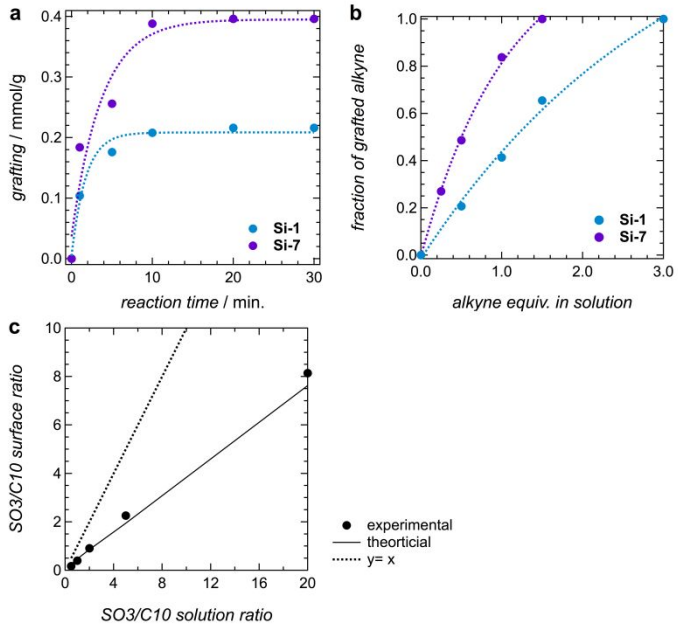

Figure 1. (a) Grafting kinetics of alkynes **1** and **7** (1.2 equiv.) on azide silica. (b) Fraction of grafted alkyne as a function of the equivalents of **1** and **7**, respectively. The lines are exponential fits. (c) SO_3/C_{10} surface ratio in bifunctional mixed silicas **Si-sim-x** as a function of the solution ratio. The continuous line is a linearly-additive model of surface partition based on the data in panel (b). The dashed line indicates identical surface and solution ratios.

Sequential grafting

Although the simultaneous grafting is a very interesting approach because it limits the number of reaction steps and subsequent purifications, and allows to accurately set final surface ratios, the moderate grafting efficiency prompted us to investigate an original sequential grafting strategy. Precisely, we prepared a series of sulfonic acid silicas **Si-1-x** by reacting azide silica **Si-N_3** with alkyne **1** in limiting amount relative to the azide

loading as determined in Figure 1b (with x the number of equivalents of alkyne **1**), thus leaving some surface azide groups available. The latter are then capped with excess of the secondary hydrophobic alkyne **7** under non-aqueous CuAAC conditions, yielding bifunctional mixed silicas **Si-seq-x** (Scheme 4).

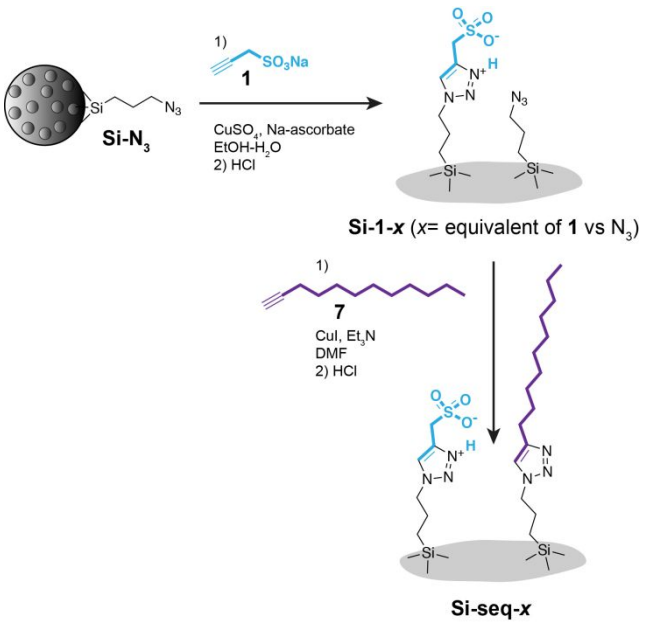

Scheme 4. Sequential preparation of bifunctional mixed SO_3/C_{10} silica.

Similarly to silicas **Si-sim-x** prepared via a simultaneous grafting, the obtained surface ratios were determined by IEC and TGA after each CuAAC step (Table 3). Noteworthy, this time, almost quantitative grafting could be achieved. DTG confirmed the controlled grafting of the propargylsulfonate as evidenced by thermal events corresponding to the grafted sulfonates (350°C) and the residual azides (250°C) in different proportions as a function of the number of equivalents x of alkyne **1** used relative to the azide loading (Figure S3). DTG also confirmed the efficiency of the final CuAAC step with 1-dodecyne through the disappearance of the thermal event corresponding to the azide layer (250°C) along with the appearance of the thermal event corresponding to the decyl layer (400°C) (Figure S3). In parallel, FT-IR evidenced the presence of residual azide groups (2100 cm^{-1}) after the first grafting that disappeared following the second CuAAC step (Figure S7).

Table 3. Determination of surface ratios for silicas **Si-step-*x***.

Silica	Equiv.of **1**	IEC for **Si-1** (mmol H^+/g)	Total organic loading (mmol/g)	SO_3/C_{10} surface ratio	Total grafting efficiency (%)
Si-N_3	-	0.04	0.37	-	-
Si-seq-0.5	0.5	0.10	0.37	0.19	100
Si-seq-1.0	1.0	0.19	0.33	0.57	89
Si-seq-1.5	1.5	0.23	0.34	1.26	92

Pairing

As we recently reported,[27] our CuAAC approach allows pairing the sulfonic group with secondary functions by means of the triazole linker. Hence, bifunctional silica **Si-paired** with paired sulfonic acid and decyl groups was prepared from silica **Si-1** obtained by the quantitative CuAAC reaction of azide silica with propargylsulfonate **1**. **Si-1** was subsequently treated with excess 1-iododecane in presence of *N*,*N*'-diisopropylethylamine (DIPEA) to afford the paired SO_3H/C_{10} silica **Si-paired** (Scheme 5).

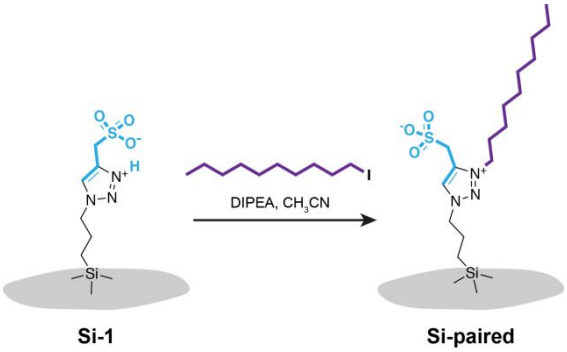

Scheme 5. Preparation of bifunctional paired SO_3/C_{10} silica from **Si-1**.

TGA confirmed the quantitative CuAAC and substitution steps, thus resulting in a 1:1 SO_3H/C_{10} surface ratio in **Si-paired**.[27] IEC analysis also confirmed the zwitterionic nature of **Si-paired**, with a proton loading of 0.04 mmol/g corresponding to residual silanols as measured for azide-funtionalized silica **Si-N_3** (Table 2).[27]

Catalysis

As observed in our previous report,[27] the slightly basic triazole ring in this system traps the sulfonic acid proton (as depicted in Schemes 3 and 4), depleting its catalytic activity. In order to circumvent this, it is necessary to mask the nitrogen ring by alkylation (as in **Si-paired**, Scheme 5), or by protonation. Here, all the zwitterionic silica catalysts **Si-sim-x**, **Si-seq-x** and the **Si-paired** were thus treated with stoichiometric amount of triflic acid (TfOH, 1.05 equiv. relative to the triazole loading) prior to catalysis, resulting in the general mixed and paired active catalysts shown in Scheme 1. This treatment was also performed for the monofunctional SO_3H- and C_{10}-functionalized silicas **Si-1** and **Si-7**, respectively, to test the catalytic contribution of each individual site. The obtained hybrid catalysts were characterized by TGA, FT-IR, XPS, elemental analysis, IEC, potentiometric titration and nitrogen physisorption (Supporting Information). Especially, XPS showed the shifting of the N 1s XPS signals towards higher binding energies following treatment with TfOH (Figures S12, S14 and S16, Table S1), confirming the protonation of the triazole ring. The presence of the triflate anion was confirmed by the appearance of a F 1s signal at ca. 688 eV together with an high-energy C 1s component at ca. 292 eV (Figure S13-S16, Table S1). IEC measurements attested the increase of the proton loading following TfOH treatment as expected (Table S3). The obtained values were consistent with the theoretical proton loading calculated from the initial triazole loading and starting IEC (Table S3), thus confirming the full protonation of the triazoles. Elemental analyses (Table S2) are also in good agreement with the expected values. Potentiometric titration with *n*-butylamine (Figure S17) provided an assessment of the acidity strength by comparing the value of the initial electrode potential E_i.[40] Noteworthy, the paired catalyst **Si-paired** exhibited the highest E_i value of 660 mV, much higher than that of a commercial Si-Pr-SO_3H (430 mV) (Figure 2). Additionally, slight differences in E_i values were observed for the mixed-type catalysts, **Si-sim-*x*** and **Si-seq-*x***, which were lower than the paired catalyst but higher than a commercial sulfonic acid silica. **Si-1** showed an E_i value of 633 mV, close to that of **Si-paired**, while a lowest value of 411 mV was measured for **Si-7**.

All the catalysts were evaluated in the model esterification of octanol with acetic acid (Scheme 1, Figures S18-S20) and the activity is illustrated in Figure 2 as a function of the relative surface composition (-N_3, -SO_3 and -C_{10}) of the catalyst. Remarkably, **Si-paired** showed the highest activity, with an initial reaction rate k 6-times higher than the

commercial propylsulfonic acid silica. The reaction rates for the mixed catalyst, **Si-sim-x** and **Si-seq-x**, remain 2- to 4-times slower than with **Si-paired**. The monofunctional sulfonic acid catalyst **Si-1** showed an initial reaction rate of 0.21 mmol.min^{-1}, on average comparable to that of the mixed catalysts. **Si-7** showed an activity similar to that of the commercial silica, consistent with their similar E_i. It is also interesting to note that the initial reaction rates closely follow the measured acidity strengths (E_i) (Figure 2, Figure S21).

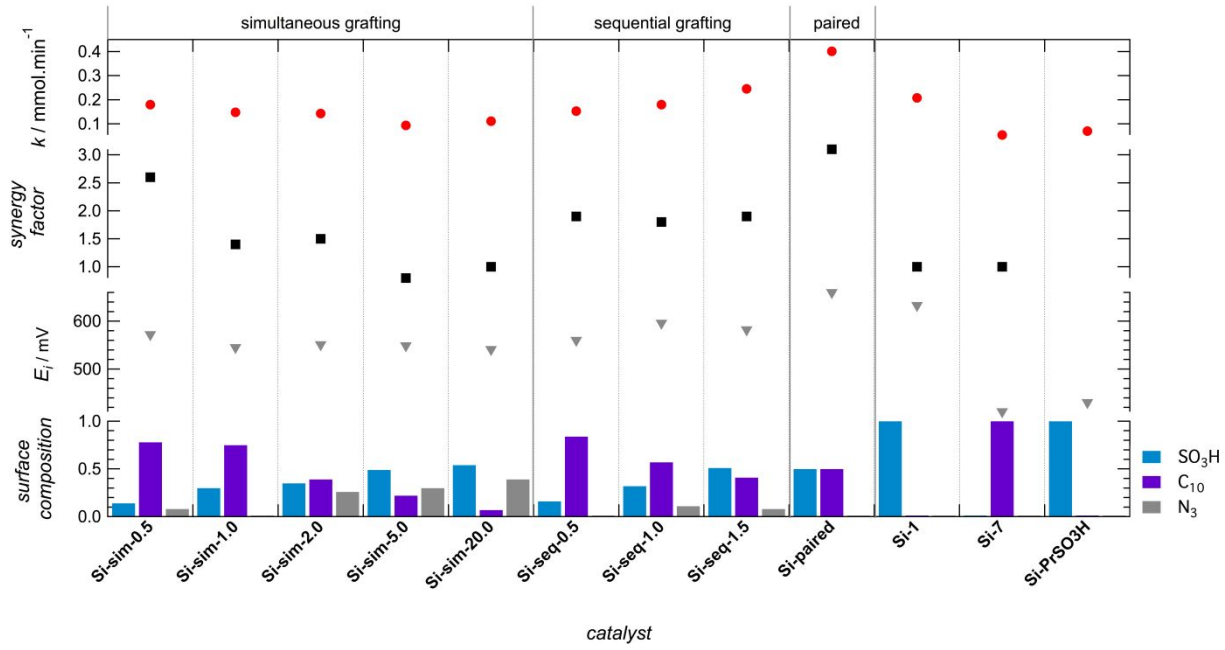

Figure 2. Catalytic activity (initial rate constant k and synergy factor SF) of supported catalysts **Si-sim-x**, **Si-seq-x**, **Si-paired**, **Si-1** and **Si-7** in the esterification of n-octanol with acetic acid as a function of surface composition and initial electrode potential E_i.

The effect of composition in the mixed catalysts shows a different trend depending on whether the catalysts are prepared via a simultaneous or sequential post-modification approach. In the simultaneous grafting method, the activity tends to increase with the increase of the hydrophobic C_{10} fraction. However, for the catalysts prepared via the sequential approach, the tendency seems to be reverse: the activity decreases with the increase of the C_{10} components. Yet, it is important to note that the mixed catalysts **Si-sim-x** show incomplete grafting, with an important fraction of azide remaining on the surface that most probably limits the synergy between the decyl and sulfonic acid

groups, while the sequential **Si-seq-x** catalysts show an almost complete grafting and their activity tend towards that of the paired catalyst **Si-paired** (i.e., 1:1 SO_3H/C_{10} surface ratio). It still remains difficult to compare the mixed catalysts and the paired one because of the random distribution of the active sites in the former. It is however clear that the paired catalyst, having the complementary sites coupled together is significantly more efficient.

Knowing the relative surface composition of all the bifunctional catalysts, and the intrinsic activity of the SO_3H- and C_{10}-triazolium catalysts **Si-1** and **Si-7**, respectively, it is possible to calculate a synergy factor *SF* for each catalyst that compares the measured activity when the two groups are mixed together on the same surface (comprising thus combined sites from **Si-1** and **Si-7**) with that of the two groups operating separately. This synergy factor *SF* is determined here as the ratio between the measured initial reaction rate *k* and the calculated rate from the intrinsic rate of **Si-1** ($k_{Si\text{-}1}$) and **Si-7** ($k_{Si\text{-}7}$) corrected by their surface ratio for a given mixed catalyst:

$$SF = {}^{k}/(x\mathrm{SO}_3 \times k_{\mathrm{Si}\,\text{-}\,1} + x\mathrm{C}_{10} \times k_{\mathrm{Si}\,\text{-}\,7})$$

with $x\mathrm{SO}_3$ and $x\mathrm{C}_{10}$ being the molar fractions of the $-SO_3$ and $-C_{10}$ groups on surface for the studied catalyst.

This factor provides another way to compare the mixed catalysts (Figure 2) and shows a remarkable synergistic effect for catalyst **Si-sim-0.5** with a *SF*= 2.6. For the simultaneous mixed catalysts **Si-sim-x**, the *SF* rapidly drops to ca. 1 (no synergy) with increasing the surface molar fraction of $-SO_3$ sites, suggesting that the $-SO_3$ and $-C_{10}$ sites behave as being isolated one to another. Hence, it is more likely that this grafting method yields phase segregation of the sulfonic and decyl sites; yet, for very low SO_3H contents (*e.g.*, **Si-sim-0.5**), the sulfonic acid sites are drown into a C_{10} layer and benefit from its hydrophobicity. This surface partitioning is more likely due to the strong van der Waals interactions between the decyl chains, thus rapidly creating islands of **7** on surface.

The sequential mixed catalysts **Si-seq-x** show a *SF* of 1.9, independent of the tested relative surface compositions, suggesting a good intermixing of the two components in the monolayer. Indeed, contrary to the simultaneous approach, the stepwise grafting

allows achieving a uniform random distribution of the active sites as there is no supramolecular interaction driving the clustered grafting of **1**, contrarily to **7**. This however remains inferior to the case of **Si-paired** (*SF*= 3.1) for which perfect pairing between acidic and hydrophobic groups results in maximal synergy and catalytic efficiency. Catalyst **Si-paired** was previously shown to be reusable for at least 5 runs without significant loss of activity in the esterification of octanol with acetic acid.[27]

Therefore, beyond controlling the relative surface ratio of functional groups, it is critical to master their relative distribution on surface to achieve maximum synergistic effects. In the present case, the hydrophobic sites are facilitating the adsorption and transfer of the hydrophobic reactant to the active sites by enhancing the wettability of the solid catalyst towards octanol.[41] Additionally, it is very likely that the hydrophobicity allows shifting reaction equilibrium by removing the water products from the active sites,[42] this also contributing to the improvement of catalyst activity and stability as water is not interfering with the catalytic sulfonic acid sites. Hence, an efficient intermixing of the acidic and hydrophobic groups is central for rate acceleration. Moreover, synergistic effects are also depending on the proximity of the complementary groups – especially when the two groups are involved in the same catalytic cycle – that is mainly governed by the grafting density[34] of the organic layer and pore size[43] of the siliceous support. Nonetheless, grafting density is often not homogeneous and large local variations can be observed within a catalyst, especially when using post-functionalization approaches,[33, 44-49] which render difficult the interpretation on the effect of grafting density. Although the proximity parameter is less critical in the present case since the hydrophobic groups are not involved in the catalytic cycle, a minimum grafting density is necessary to ensure sufficient surface hydrophobicity and enable efficient adsorption and transfer of octanol to the catalytic sulfonic acid sites.

Hence, our approach consisting on pairing the complementary sites on surface allows circumventing both the effects of uneven distribution and grafting density often associated with mixed-monolayer catalysts.

CONCLUSIONS

Understanding and controlling how functional groups are distributed on surface is critical to design efficient heterogeneous multifunctional cooperative and synergistic catalytic systems. Here, we presented different post-functionalization methods to

prepare bifunctional supported catalysts bearing sulfonic acid sites and hydrophobic chains. The mixed monolayer catalysts showed different spatial distributions of the functional groups on surface (segregated/clustered or mixed) depending on whether they are prepared by a simultaneous or stepwise CuAAC-grafting on azide-functionalized silica, respectively. Provided a good mixing of the components is achieved, important catalytic synergistic effects can be observed. Yet, random or uneven distribution prevents full synergy to be expressed. We further demonstrated that pairing the sulfonic acid sites with the hydrophobic decyl chains, unique to our CuAAC grafting approach, provided unequalled catalytic activity as a result of strong synergistic effects resulting from the organized distribution.

This work highlights the importance of the spatial distribution of functional groups in supported cooperative/synergistic catalysis and provides tools and unique design principles for the next-generation multifunctional hybrid catalysts.

ACKNOWLEDGEMENT

The authors acknowledge the European Regional Development Fund (ERDF) and Wallonia (Operational Program "Wallonia-2020.EU"), and the Région wallonne-DG06 (Beware “Friedelcat” project n°1510459). Authors also acknowledge the “Communauté française de Belgique” for the financial support through the ARC programme (15/20-069). Cécile d’Haese and Claudine Givron are acknowledged for XPS and elementary analysis measurements, respectively.

REFERENCES

1. Liu, F.; Huang, K.; Zheng, A.; Xiao, F.-S.; Dai, S., Hydrophobic Solid Acids and Their Catalytic Applications in Green and Sustainable Chemistry. *ACS Catal.* **2018,** *8* (1), 372-391.

2. Sun, Q.; Wang, S.; Aguila, B.; Meng, X.; Ma, S.; Xiao, F.-S., Creating solvation environments in heterogeneous catalysts for efficient biomass conversion. *Nat. Commun.* **2018,** *9* (1), 3236.

3. Corma, A.; Domine, M.; A. Gaona, J.; L. Jorda, J.; T. Navarro, M.; Rey, F.; Perez-Pariente, J.; Tsuji, J.; McCulloch, B.; T. Nemeth, L., Strategies to improve the epoxidation activity and selectivity of Ti-MCM-41. *Chem. Commun.* **1998,** (20), 2211-2212.

4. M. Van Rhijn, W.; E. De Vos, D.; F. Sels, B.; D. Bossaert, W., Sulfonic acid functionalised ordered mesoporous materials as catalysts for condensation and esterification reactions. *Chem. Commun.* **1998,** (3), 317-318.

5. Tatsumi, T.; A. Koyano, K.; Igarashi, N., Remarkable activity enhancement by trimethylsilylation in oxidation of alkenes and alkanes with H2O2 catalyzed by titanium-containing mesoporous molecular sieves. *Chem. Commun.* **1998,** (3), 325-326.
6. Díaz, I.; Márquez-Alvarez, C.; Mohino, F.; Pérez-Pariente, J. n.; Sastre, E., Combined Alkyl and Sulfonic Acid Functionalization of MCM-41-Type Silica. *J. Catal.* **2000,** *193* (2), 295-302.
7. Díaz, I.; Márquez-Alvarez, C.; Mohino, F.; Pérez-Pariente, J. n.; Sastre, E., Combined Alkyl and Sulfonic Acid Functionalization of MCM-41-Type Silica: Part 1. Synthesis and Characterization. *J. Catal.* **2000,** *193* (2), 283-294.
8. Mbaraka, I. K.; Shanks, B. H., Design of multifunctionalized mesoporous silicas for esterification of fatty acid. *J. Catal.* **2005,** *229* (2), 365-373.
9. Karimi, B.; Zareyee, D., Design of a Highly Efficient and Water-Tolerant Sulfonic Acid Nanoreactor Based on Tunable Ordered Porous Silica for the von Pechmann Reaction. *Org. Lett.* **2008,** *10* (18), 3989-3992.
10. Dacquin, J.-P.; Cross, H. E.; Brown, D. R.; Duren, T.; Williams, J. J.; Lee, A. F.; Wilson, K., Interdependent lateral interactions, hydrophobicity and acid strength and their influence on the catalytic activity of nanoporous sulfonic acid silicas. *Green Chem.* **2010,** *12* (8), 1383-1391.
11. Karimi, B.; Mirzaei, H. M., The influence of hydrophobic/hydrophilic balance of the mesoporous solid acid catalysts in the selective dehydration of fructose into HMF. *RSC Adv.* **2013,** *3* (43), 20655-20661.
12. Manayil, J. C.; dos Santos, V. C.; Jentoft, F. C.; Granollers Mesa, M.; Lee, A. F.; Wilson, K., Octyl Co-grafted PrSO3H/SBA-15: Tunable Hydrophobic Solid Acid Catalysts for Acetic Acid Esterification. *ChemCatChem* **2017,** *9* (12), 2231-2238.
13. Sayari, A.; Hamoudi, S., Periodic Mesoporous Silica-Based Organic-Inorganic Nanocomposite Materials. *Chem. Mater.* **2001,** *13* (10), 3151-3168.
14. Hunks, W. J.; Ozin, G. A., Challenges and advances in the chemistry of periodic mesoporous organosilicas (PMOs). *J. Mater. Chem.* **2005,** *15* (35-36), 3716-3724.
15. Hoffmann, F.; Cornelius, M.; Morell, J.; Froeba, M., Periodic mesoporous organosilicas (PMOs): past, present, and future. *J. Nanosci. Nanotechnol.* **2006,** *6* (2), 265-288.
16. Yang, Q.; Liu, J.; Zhang, L.; Li, C., Functionalized periodic mesoporous organosilicas for catalysis. *J. Mater. Chem.* **2009,** *19* (14), 1945-1955.
17. Van Der Voort, P.; Esquivel, D.; De Canck, E.; Goethals, F.; Van Driessche, I.; Romero-Salguero, F. J., Periodic Mesoporous Organosilicas: from simple to complex bridges; a comprehensive overview of functions, morphologies and applications. *Chem. Soc. Rev.* **2013,** *42* (9), 3913-3955.
18. Esquivel, D.; De Canck, E.; Jimenez-Sanchidrian, C.; Van Der Voort, P.; Romero-Salguero, F. J., Periodic Mesoporous Organosilicas as Catalysts for Organic Reactions. *Curr. Org. Chem.* **2014,** *18* (10), 1280-1295.
19. Manayil, J. C.; Lee, A. F.; Wilson, K., Functionalized periodic mesoporous organosilicas: tunable hydrophobic solid acids for biomass conversion. *Molecules* **2019,** *24* (2), 239/1-239/25.
20. Yang, Q.; Liu, J.; Yang, J.; Kapoor, M. P.; Inagaki, S.; Li, C., Synthesis, characterization, and catalytic activity of sulfonic acid-functionalized periodic mesoporous organosilicas. *J. Catal.* **2004,** *228* (2), 265-272.
21. Yang, Q.; Kapoor, M. P.; Inagaki, S.; Shirokura, N.; Kondo, J. N.; Domen, K., Catalytic application of sulfonic acid functionalized mesoporous benzene–silica with crystal-like pore wall structure in esterification. *J. Mol. Catal. A: Chem.* **2005,** *230* (1), 85-89.

22. Yang, Q.; Kapoor, M. P.; Shirokura, N.; Ohashi, M.; Inagaki, S.; Kondo, J. N.; Domen, K., Ethane-bridged hybrid mesoporous functionalized organosilicas with terminal sulfonic groups and their catalytic applications. *J. Mater. Chem.* **2005,** *15* (6), 666-673.
23. Rác, B.; Hegyes, P.; Forgo, P.; Molnár, Á., Sulfonic acid-functionalized phenylene-bridged periodic mesoporous organosilicas as catalyst materials. *Appl. Catal., A* **2006,** *299*, 193-201.
24. Rat, M.; Zahedi-Niaki, M. H.; Kaliaguine, S.; Do, T. O., Sulfonic acid functionalized periodic mesoporous organosilicas as acetalization catalysts. *Microporous Mesoporous Mater.* **2008,** *112* (1), 26-31.
25. Karam, A.; Alonso, J. C.; Gerganova, T. I.; Ferreira, P.; Bion, N.; Barrault, J.; Jérôme, F., Sulfonic acid functionalized crystal-like mesoporous benzene–silica as a remarkable water-tolerant catalyst. *Chem. Commun.* **2009,** (45), 7000-7002.
26. Manayil, C. J.; Lee, F. A.; Wilson, K., Functionalized Periodic Mesoporous Organosilicas: Tunable Hydrophobic Solid Acids for Biomass Conversion. *Molecules* **2019,** *24* (2).
27. Kasinathan, P.; Lang, C.; Radhakrishnan, S.; Schnee, J.; D'Haese, C.; Breynaert, E.; Martens, J. A.; Gaigneaux, E. M.; Jonas, A. M.; Fernandes, A. E., "Click" Silica-Supported Sulfonic Acid Catalysts with Variable Acid Strength and Surface Polarity. *Chem. Eur. J.* **2019,** *25* (27), 6753-6762.
28. Margelefsky, E. L.; Zeidan, R. K.; Dufaud, V.; Davis, M. E., Organized Surface Functional Groups: Cooperative Catalysis via Thiol/Sulfonic Acid Pairing. *J. Am. Chem. Soc.* **2007,** *129* (44), 13691-13697.
29. Margelefsky, E. L.; Zeidan, R. K.; Davis, M. E., Cooperative catalysis by silica-supported organic functional groups. *Chem. Soc. Rev.* **2008,** *37* (6), 1118-1126.
30. Margelefsky, E. L.; Bendjériou, A.; Zeidan, R. K.; Dufaud, V.; Davis, M. E., Nanoscale Organization of Thiol and Arylsulfonic Acid on Silica Leads to a Highly Active and Selective Bifunctional, Heterogeneous Catalyst. *J. Am. Chem. Soc.* **2008,** *130* (40), 13442-13449.
31. Nakazawa, J.; Smith, B. J.; Stack, T. D. P., Discrete Complexes Immobilized onto Click-SBA-15 Silica: Controllable Loadings and the Impact of Surface Coverage on Catalysis. *J. Am. Chem. Soc.* **2012,** *134* (5), 2750-2759.
32. Dau, P. V.; Cohen, S. M., A Bifunctional, Site-Isolated Metal–Organic Framework-Based Tandem Catalyst. *Inorg. Chem.* **2015,** *54* (7), 3134-3138.
33. Smith, B. J.; Hernández Gallegos, P. A.; Butsch, K.; Stack, T. D. P., Metal complex assembly controlled by surface ligand distribution on mesoporous silica: Quantification using refractive index matching and impact on catalysis. *J. Catal.* **2016,** *335*, 197-203.
34. Noda, H.; Motokura, K.; Wakabayashi, Y.; Sasaki, K.; Tajiri, H.; Miyaji, A.; Yamaguchi, S.; Baba, T., Direct Estimation of the Surface Location of Immobilized Functional Groups for Concerted Catalysis Using a Probe Molecule. *Chem. Eur. J.* **2016,** *22* (15), 5113-5117.
35. Chandra, P.; Jonas, A. M.; Fernandes, A. E., Spatial Coordination of Cooperativity in Silica-Supported Cu/TEMPO/Imidazole Catalytic Triad. *ACS Catal.* **2018,** *8* (7), 6006-6011.
36. Chandra, P.; Jonas, A. M.; Fernandes, A. E., Sequence and Surface Confinement Direct Cooperativity in Catalytic Precision Oligomers. *J. Am. Chem. Soc.* **2018,** *140* (15), 5179-5184.
37. Fernandes, A. E.; Jonas, A. M., Design and engineering of multifunctional silica-supported cooperative catalysts. *Catal. Today* **2019,** *334*, 173-186.

38. Fernandes, A. E.; Riant, O.; Jonas, A. M.; Jensen, K. F., One "Click" to controlled bifunctional supported catalysts for the Cu/TEMPO-catalyzed aerobic oxidation of alcohols. *RSC Adv.* **2016,** *6* (43), 36602-36605.
39. Fernandes, A. E.; Riant, O.; Jensen, K. F.; Jonas, A. M., Molecular Engineering of Trifunctional Supported Catalysts for the Aerobic Oxidation of Alcohols. *Angew. Chem. Int. Ed.* **2016,** *55* (37), 11044-11048.
40. Song, K.; Zhang, H.; Zhang, Y.; Tang, Y.; Tang, K., Preparation and characterization of WOx/ZrO2 nanosized catalysts with high WOx dispersion threshold and acidity. *J. Catal.* **2013,** *299*, 119-128.
41. Wang, L.; Xiao, F.-S., The Importance of Catalyst Wettability. *ChemCatChem* **2014,** *6* (11), 3048-3052.
42. Tsai, C.-H.; Chen, H.-T.; Althaus, S. M.; Mao, K.; Kobayashi, T.; Pruski, M.; Lin, V. S. Y., Rational Catalyst Design: A Multifunctional Mesoporous Silica Catalyst for Shifting the Reaction Equilibrium by Removal of Byproduct. *ACS Catal.* **2011,** *1* (7), 729-732.
43. Motokura, K.; Ikeda, M.; Nambo, M.; Chun, W.-J.; Nakajima, K.; Tanaka, S., Concerted Catalysis in Tight Spaces: Palladium-Catalyzed Allylation Reactions Accelerated by Accumulated Active Sites in Mesoporous Silica. *ChemCatChem* **2017,** *9* (15), 2924-2929.
44. Lim, M. H.; Stein, A., Comparative Studies of Grafting and Direct Syntheses of Inorganic–Organic Hybrid Mesoporous Materials. *Chem. Mater.* **1999,** *11* (11), 3285-3295.
45. Stein, A.; Melde, B. J.; Schroden, R. C., Hybrid Inorganic–Organic Mesoporous Silicates—Nanoscopic Reactors Coming of Age. *Adv. Mater.* **2000,** *12* (19), 1403-1419.
46. Corriu, R. J. P.; Lancelle-Beltran, E.; Mehdi, A.; Reyé, C.; Brandès, S.; Guilard, R., Ordered mesoporous hybrid materials containing cobalt(ii) Schiff base complex. *J. Mater. Chem.* **2002,** *12* (5), 1355-1362.
47. Mouawia, R.; Mehdi, A.; Reye, C.; Corriu, R. J. P., Bifunctional ordered mesoporous materials: direct synthesis and study of the distribution of two distinct functional groups in the pore channels. *J. Mater. Chem.* **2008,** *18* (35), 4193-4203.
48. Sharifi, M.; Marschall, R.; Wilhelm, M.; Wallacher, D.; Wark, M., Detection of Homogeneous Distribution of Functional Groups in Mesoporous Silica by Small Angle Neutron Scattering and in Situ Adsorption of Nitrogen or Water. *Langmuir* **2011,** *27* (9), 5516-5522.
49. Conley, M. P.; Copéret, C.; Thieuleux, C., Mesostructured Hybrid Organic–Silica Materials: Ideal Supports for Well-Defined Heterogeneous Organometallic Catalysts. *ACS Catal.* **2014,** *4* (5), 1458-1469.

Table of content artwork